IEEE Access
Multidisciplinary | Rapid Review | Open Access Journal

Received 18 June 2023, accepted 13 July 2023, date of publication 18 July 2023, date of current version 26 July 2023.

Digital Object Identifier 10.1109/ACCESS.2023.3296615

RESEARCH ARTICLE

A Novel Indoor Tracking Method Based on IMM-MLKF With CSI Measurements

WENXU WANG AND YINGBIAO JIA
School of Information Engineering, Shaoguan University, Shaoguan 512005, China
Corresponding author: Wenxu Wang (wangwenxu0909@126.com)

This work was supported in part by the Shaoguan University Doctoral Research Startup Fund under Grant 441-9900064601, and in part by the Guangdong Key Construction Discipline Research Capacity Enhancement Project under Grant 2022ZDJS049 and Grant 2022ZDJS048.

ABSTRACT Indoor target tracking based on Wi-Fi signals entails the integration of both the target motion model and the measurement model. However, a single motion model is inadequate to match the changing motion state of the target at each moment, and linearization of the measurement model may introduce additional errors. To tackle these problems, we propose a localization method called IMM-MLKF. For the measurement equation, we adopt the fingerprinting model to perform maximum likelihood estimation on the target, obtaining the mean and covariance matrix of the target state distribution. This method eliminates the error introduced by linearization. For the motion equation, multiple models are used for parallel computation. The likelihood function values generated by each model from the measurements are used as their model confidences, enabling the combining model to match the motion of the target. We validated the method in two different scenarios using channel state information as the fingerprint feature. Our results show that compared with similar Bayesian filtering methods based on interactive multiple models, this method has superior tracking accuracy. Additionally, this method's operating efficiency is higher than particle filtering methods.

INDEX TERMS Indoor tracking, multiple model, maximum likelihood estimation, channel state information.

I. INTRODUCTION

The advancements in mobile communication and internet technologies have significantly enhanced convenience in people's daily lives. Location-based services (LBS) have become an important aspect of people's intelligent life, and its fundamental challenge is to use wireless communication networks or positioning methods to acquire the current location of the target device. In terms of positioning scenes, positioning technology can be classified into two categories, namely indoor positioning and outdoor positioning. At present, the global positioning system (GPS) is generally used for outdoor positioning [1]. However, the complex indoor environment and the obstacles in it cause the attenuation and multipath effect of wireless signals, which makes it impossible to find a solution for all indoor scenarios. Therefore, a variety of wireless signals are applied to different positioning problems, such as Wi-Fi [2], Bluetooth [3], ZigBee [4], Radio Frequency Identification Device (RFID) [5], Ultra-wide Band (UWB) [6], and visible light [7]. Since most smartphones, laptops, and other portable mobile devices are equipped with Wi-Fi chips, the cost of Wi-Fi positioning solutions is greatly reduced [8], making Wi-Fi the most popular and promising positioning technology.

Generally speaking, indoor location methods can be divided into two categories: geometric mapping and fingerprinting [9]. Geometric mapping calculates the relative geometric information, such as distance and angle, between the target position and the reference position using received signals [10]. Geometric methods, such as trilateral positioning, are then used to estimate the position of the target. The reliability of the geometric mapping method depends heavily on the reception of the line of sight (LOS) signal [11], and the indoor multi-path effect can seriously affect the positioning accuracy. Fingerprinting methods collect signal features from all positions in the environment to create a fingerprint database. These methods transform the location problem into a matching problem between the signal features collected at the location and the fingerprints in the database. The performance of the fingerprinting method depends on the signal

The associate editor coordinating the review of this manuscript and approving it for publication was Xueqin Jiang.

differentiation between different positions [12]. However, a disadvantage of fingerprinting methods is that they require additional work to build a database, and the fingerprint database needs to be updated when the environment changes.

In wireless localization systems, there are many signal indicators that can be used for positioning, including time of arrival (TOA), time difference of arrival (TDOA), round trip time (RTT), angle of arrival (AOA), received signal strength indicator (RSSI), channel state information (CSI), etc. Among them, TOA, TDOA, RTT, and AOA can be converted into information about the distance or angle between the target and the wireless access point (AP), and the target's location can be estimated through geometric mapping; while in the fingerprinting localization process, RSSI and CSI are the most commonly used positioning indicators to explore differences between different locations [13]. Although RSSI is easy to obtain, it is susceptible to the accumulation of multipath signals, and can only roughly estimate the position. CSI, on the other hand, includes amplitude and phase information of all subcarriers in the transmission signal and can provide higher accuracy in determining location compared to RSSI [14]. Therefore, CSI-based indoor positioning has a higher theoretical upper limit than RSSI-based methods.

In most localization scenarios, it's important to obtain real-time position information of moving objects. Current real-time target tracking methods are largely based on Bayesian filtering [15], which combines prior information and measurement information probabilistically. At each sampling time point, the position estimate is updated by fusing signal and target motion information. Most Wi-Fi based target tracking methods use the information obtained by other sensors to improve the positioning accuracy, such as UWB sensors [16], inertial sensors [17] and landmarks [18].

The main principle of Bayesian filtering for tracking is to fuse the information contained in the target's motion state with the information obtained by the sensors. Once the system's state equation and measurement equation are established, the posterior probability density function (PDF) of the system state can be recursively calculated through Bayesian filtering to achieve an estimation of the target state. If these two equations do not meet the conditions of linearity and Gaussianity, approximate methods need to be used to simplify them, which can be divided into two categories: one category of the approximation methods does not require explicit constraints on the posterior PDF, and the most commonly used method among them is particle filtering (PF) [19]. Particle filtering uses the method of stochastic importance sampling to approximate the posterior probability density function, which effectively deals with nonlinear problems and avoids the assumption of Gaussianity about the system. However, the estimation accuracy of PF depends on the number of particles, and the time and space complexity increases as the number of particles increases [20]. The other type of approximation method requires a Gaussianity assumption for the posterior probability density function. Based on the linear minimum variance estimation criterion, different nonlinear filtering methods are formed according to different numerical calculation methods, such as extended Kalman filtering (EKF) [21], unscented Kalman filtering (UKF) [22], and cubature Kalman filter (CKF) [23] etc.

In addition, the methods mentioned above only apply to fixed motion models. Once the target's maneuvering mode changes, it will bring serious errors to the tracking result. Obviously, using a single model for target tracking can no longer meet the tracking requirements at this time. Therefore, the multiple model (MM) algorithm was developed [24]. Currently, the best multiple model algorithm is the interactive multiple model (IMM) algorithm [25]. This algorithm uses a set of models, obtains model likelihood functions based on the innovation between prediction and measurement, and computes the target position according to the feedback likelihood function. The IMM algorithm is often combined with algorithms such as EKF [26], UKF [27] and CKF [28], and can improve the accuracy of positioning in appropriate scenarios.

In this paper, a new target tracking algorithm based on Bayesian filtering and IMM is proposed, which is combined with CSI fingerprint positioning. We establish a fingerprint model of CSI and use the maximum likelihood estimation method to obtain the static positioning result of the target. Then, multiple filters are established in parallel for different motion models, and the model probability is updated based on the model matching likelihood function. The position of the target is obtained by combining the modified state estimation values of all filters. The static positioning process of maximum likelihood estimation fully utilizes the location information contained in the CSI signal, and the parallel calculation of multiple linear motion models can better predict the target's motion trajectory while ensuring efficiency. In summary, the main contribution of this paper is to effectively combine CSI fingerprint positioning, IMM, and Bayesian filtering, match suitable motion models for different motion states of the target, and efficiently integrate with the information provided by CSI through maximum likelihood Kalman filtering. The experimental results in this paper show that compared with other similar methods, the proposed method can balance computational efficiency and positioning accuracy.

The structure of this paper is outlined as follows. Section II reviewed the related work on CSI-based fingerprint localization and Bayesian filtering. Section III outlines the positioning problem. The innovative localization method is outlined in Section IV. In Section V, we present numerical evidence demonstrating the benefits of the proposed method. Finally, the paper concludes with final remarks in Section VI.

II. RELATED WORK

A. CSI FINGERPRINTING METHODS

CSI is a kind of fine-grained channel response information obtained in communication systems under the orthogonal frequency division multiplexing (OFDM) protocol. It includes

attenuation information of the signal on each transmission path. CSI is represented as channel impulse response (CIR) and channel frequency response (CFR) in the time domain and frequency domain, respectively. The channel frequency response can be expressed as

$$Y = HX + N, \tag{1}$$

where X is the transmission signal vector, Y is the received signal vector, N is the channel noise matrix, and H represents a complex matrix that includes channel state information. By collecting the information of the H matrix at different locations, a fingerprint database can be established.

After the fingerprint database is established, the positioning problem is transformed into a matching problem between the received signal and the information stored in the fingerprint database. This matching process requires the use of positioning algorithms, such as k-nearest neighbor (KNN) [29], support vector machine (SVM) [30], and linear discriminant analysis [31]. Compared to these methods, deep learning-based Wi-Fi positioning methods can automatically filter out the irrelevant information in the raw signals that is not useful for positioning, extract reliable features, and achieve better positioning accuracy and robustness in complex indoor environments. Wang et al. [32] proposed a deep learning-based indoor positioning method called DeepFi. This method uses a deep neural network with 7 hidden layers to classify data obtained from an AP with 3 antennas. Qin et al. [33] proposed a positioning method called CADE-CNN positioning (CCPos), which utilizes a convolutional denoising autoencoder (CDAE) to denoise the signals and extract key features, followed by a convolutional neural network (CNN) to output the location estimation.

However, if positioning is treated as a classification problem, only discrete positioning results can be obtained and their accuracy depends on the number of fingerprints collected during the initialization phase. To address these problems, some regression-based positioning algorithms have also been proposed, such as Gaussian process regression [34] and support vector regression (SVR) [35]. Once an analytical expression for the regression model, which maps location information to fingerprint signals, is found, then the localization problem can be transformed into an optimization problem, as in the method used in Section IV-B of this paper.

B. BAYESIAN FILTERING METHODS

During the positioning process at time t, we do not need to obtain the motion state of the target at all times $x_{0:t}$. We only need to obtain the current state x_t from the marginal posterior distribution $p(x_t|y_{1:t})$. Bayesian filtering is a class of recursive methods based on Bayesian theory used to calculate the value of $p(x_t|y_{1:t})$ at time t [36]. The calculation process can be divided into the following steps:

- Initialization: set the prior distribution $p(x_0)$ for the initial state;
- Prediction: estimate the state x_t of the target at time t using the previous $t-1$ observation values $y_{1:t-1}$:

$$p(x_t|y_{1:t-1}) = \int p(x_t|x_{t-1})p(x_{t-1}|y_{1:t-1})dx_{t-1}; \tag{2}$$

- Update: by using the predicted value and the newly obtained measurement value at time t, combined with the Bayes formula, we can get:

$$p(x_t|y_{1:t}) = \frac{p(y_t|x_t)p(x_t|y_{1:t-1})}{\int p(y_t|x_t)p(x_t|y_{1:t-1})dx_t}. \tag{3}$$

If both the state variables and observation variables follow normal distributions, and it is assumed that the state transition equation and measurement equation are linear functions, the Bayesian filter takes the form of Kalman filter. Otherwise, some sub-optimal nonlinear filters can be obtained through approximate methods. The simplest approximate method is to linearize the non-linear measurement equation, i.e., extend Kalman filter [37]. However, for highly non-linear systems, EKF may bring significant biases. Based on this problem, S. Julier et al. proposed the unscented Kalman filter based on the idea of unscented transformation [38]. It approximates the non-linear function using the probability density function of the state vector, producing $2n+1$ sampling points with certain weights, and then propagating through the non-linear system using these sample points, reaching the accuracy of the second-order extended Kalman filter algorithm. Compared to the EKF filtering algorithm, the UKF algorithm does not ignore the high-order terms of the Taylor series, nor does it involve solving problems with the Jacobians matrix [39]. However, as the dimension of the system increases, the UKF algorithm may result in the situation where the covariance matrix is not positive definite and cannot be filtered. To overcome the problem of low filtering accuracy of UKF in high dimensional situations, Arasaratnam and Haykin proposed the cubature Kalman filter method based on cubature integration transform [23]. This method selects a set of volume points to approximate the mean and covariance of the function, reducing the error of linearizing nonlinear functions.

Another approach for estimating the mean and covariance of the target state is particle filtering, whose principle is to use a large number of random particles to approximately represent the probability density function of the state [40]. As the number of particles increases, the approximation results become more and more accurate, but at the same time, a large amount of computational resources will be consumed. The maximum likelihood Kalman filtering (MLKF) method proposed in [41] has effectively solved this problem, and it has good handling of the nonlinearity of the measurement equation through maximum likelihood estimation, and has higher computational efficiency than particle filtering. However, this method is only applicable to a single linear motion model. Another improved algorithm named maximum likelihood particle filter (MLPF) [42] optimizes the distribution of sampled particles in particle filtering, enhancing the oper-

ational efficiency of particle filtering, but still requiring the calculation of several tens of particles for an ideal result.

However, due to the complex and diverse motion processes of targets, it is difficult to describe them using a single model. To solve this problem, the interactive multiple model was proposed [43]. The IMM algorithm uses multiple filters for parallel processing. Each filter corresponds to a different state space model, and different state space models correspond to different target maneuvering models. Therefore, each filter has a different estimate of the target state. The basic idea of the IMM algorithm is to assume that a certain model is effective at the current time, and to obtain the initial conditions of the filter that matches this specific model by mixing the estimated values of all filters at the previous time. Each model corresponds to a filter that performs parallel calculations. Finally, the model probabilities are updated based on the likelihood functions. The estimation of the IMM algorithm is a combination of estimates obtained from different models, rather than simply choosing the completely correct model estimate at each time.

Zhang et al. [26] used two extended Kalman filters for positioning in both line-of-sight and non-line-of-sight scenarios, and fused the results using the IMM algorithm. Lee et al. [27] established different motion models by analyzing different human motion patterns, such as straight-line motion, accelerated motion, and turning, and applied the IMM-UKF algorithm to track the target. Experimental results demonstrated that this method is more effective in improving localization accuracy and response speed than single-model filtering methods such as KF and PF. Radhika et al. [28] combined the IMM algorithm with CKF to propose a tracking method for highly maneuverable targets, and verified the improvement by calculating the posterior Cramér-Rao lower bound.

III. PROBLEM DESCRIPTION

Assume that the positioning environment is a two-dimensional plane ($\mathbb{R}^2$), and the target is located at $x_t \in \mathbb{R}^2$ at time t. At this time, the fingerprints obtained by the target from the Wi-Fi access point (AP) is denoted as $y_t = \left[y_t^{(1)\top}, \cdots, y_t^{(N)\top}\right]^\top$. We also assume the x_t and y_t are generated from the following model:

$$\mu_{t+1} = F\mu_t + w_t, \tag{4}$$

$$y_t = h(J\mu_t) + \iota_t. \tag{5}$$

The state $\mu_t = \left[x_t^\top, \dot{x}_t^\top\right]^\top$ consists of the position and velocity of the target at time t. The state-transition matrix is denoted by $F \in \mathbb{R}^{4\times4}$, and the process noise is represented by $w_t \sim \mathcal{N}(0, Q)$, while the measurement noise is denoted by $\iota_t \sim \mathcal{N}(0, R)$. The white process noise w_t and measurement noise ι_t are jointly independent. The selection matrix $J = [\mathcal{I}, 0]^\top$, where $\mathcal{I}$ is the identity matrix, is used such that $J\mu_t = x_t$.

Assuming that the fingerprint y_t is known but the matrix R is unknown, we can choose different matrices F and Q depending on the motion model (4). Then, the positioning problem can be formulated as follows:

Problem 1: Based on the model (4) and (5), as well as the fingerprint y_t, the problem is to solve the target's position x_t at each time $t \in \mathbb{N}$.

IV. PROPOSED METHOD

This section introduces a novel indoor positioning technique referred to as IMM-MLKF. It completes an iteration at each time t, which contains 4 stages, namely input building, maximum likelihood filtering, model probability updating and combine estimation.

A. INPUT BUILDING

Assume $\mu_{t-1}^{j,0}$ is the state value we use to predict the state at time t for the j-th model, which is composed of all r models we use in a certain proportion. $\Sigma_{t-1}^{j,0}$ is the covariance matrix and stands for the uncertainty of the model. We compute these 2 parameters as follows:

$$\mu_{t-1|t-1}^{j,0} = \sum_{i=1}^{r} \zeta_{t-1}^{i|j} \mu_{t-1|t-1}^{i}, \tag{6}$$

$$\Sigma_{t-1|t-1}^{j,0} = \sum_{i=1}^{r} \zeta_{t-1}^{i|j} [\Sigma_{t-1|t-1}^{i} + (\mu_{t-1|t-1}^{i} - \mu_{t-1|t-1}^{j,0}) \cdot \times (\mu_{t-1|t-1}^{i} - \mu_{t-1|t-1}^{j,0})^\top], \tag{7}$$

in which $\zeta_{t-1}^{i|j}$ is the mixing probability between models. The initial states and covariance matrices of each model are weighted and mixed according to the mixing probability to obtain the mixed initial state and covariance matrix. $\zeta_{t-1}^{i|j}$ can be calculated by

$$\zeta_{t-1}^{i|j} = \frac{p_{ij}\zeta_{t-1|t-1}^{i}}{\sum_{k=1}^{r} p_{kj}\zeta_{t-1|t-1}^{k}}, \tag{8}$$

where p_{ij} is the transfer probability from model i to model j.

B. MAXIMUM LIKELIHOOD FILTERING

In this stage, we use maximum likelihood Kalman filter to get the prediction and update the state value at time t. This method can deal with nonlinear measure models without increasing running time significantly [44].

1) MAXIMUM LIKELIHOOD ESTIMATION

In this step, we use the maximum likelihood estimation method based on the fingerprint model to obtain the result of static localization $\hat{x}_t$ by the current target's received fingerprint signal y_t.

$$\check{x}_t = \arg\max_x L_t(x), \tag{9}$$

$$\lambda_t = J^\top \check{x}_t, \tag{10}$$

$$\Lambda_t = J^\top \check{C}_t J, \tag{11}$$

where

$$L_t(x) = \log p\left(y_t | J\mu_t = x\right), \tag{12}$$

$$p\left(y_t|J\mu_t = x\right) = \mathcal{N}\left(y_t; \hat{h}\left(x\right), \hat{R}\right). \tag{13}$$

where $\hat{h}(x)$ is the fingerprint model we established and $\check{C}_t$ can be calculated as

$$\check{C}_t = -\nabla^2 L_t\left(\check{x}_t\right), \tag{14}$$

with $\nabla^2 L_t\left(x\right)$ representing the Hessian of L_t evaluated at x.

2) PREDICTION

The principle of this step is the same as that of the typical Kalman filter. With $\mu^{j,0}_{t-1|t-1}$ and $\Sigma^{j,0}_{t-1|t-1}$ from equation (6) and (7), we can predict the state value using the j-th motion model.

$$\mu^j_{t|t-1} = F^j_{t-1}\mu^{j,0}_{t-1|t-1}, \tag{15}$$

$$\Sigma^j_{t|t-1} = F^j_{t-1}\Sigma^{j,0}_{t-1|t-1}(F^j_{t-1})^\top + Q^j. \tag{16}$$

3) UPDATE

Since the measurement equation is nonlinear, we use the estimate $\check{x}_t$ obtained by equation (9) to get the filtering value $\mu^j_{t|t}$ and $\Sigma^j_{t|t}$.

$$\mu^j_{t|t} = \Sigma^j_{t|t}[(\Sigma^j_{t|t-1})^{-1}\mu_{t|t-1} + \Lambda_t\lambda_t], \tag{17}$$

$$\Sigma^j_{t|t} = [(\Sigma^j_{t|t-1})^{-1} - \Lambda_t]^{-1}. \tag{18}$$

C. MODEL PROBABILITY UPDATING

In this stage, we compute the likelihood value of the model to evaluate the accuracy of each model.

$$\Phi^j_t = \frac{1}{\sqrt{(2\pi)^N det(S^j_t)}} exp[-\frac{1}{2}(r^j_t)^\top (S^j_t)^{-1} r^j_t], \tag{19}$$

$$r^j_t = y_t - H_t\mu^j_{t|t-1}, \tag{20}$$

$$S^j_t = H_t\Sigma^j_{t|t-1}(H_t)^\top + R^j, \tag{21}$$

where

$$H_t = \frac{\partial h(x_t)}{\partial x_t^\top}. \tag{22}$$

Then we can get the confidence of each model

$$\xi^j_{t|t} = \frac{1}{c}\xi^j_{t|t-1}\Phi^j_t, \tag{23}$$

in which

$$\xi^j_{t|t} = \frac{1}{c}\xi^j_{t|t-1}\Phi^j_t, \tag{24}$$

in which

$$\xi^j_{t|t-1} = \sum_{i=1}^{r} p_{ij}\Phi^i_t, \tag{25}$$

$$c = \sum_{i=1}^{r}\xi^j_{t|t-1}\Phi^i_t. \tag{26}$$

$\xi^j_{t|t}$ represents the confidence that the model accurately describes the target's motion at that time. The final output of the filter is the weighted average of multiple filter estimates based on this confidence level.

D. COMBINE ESTIMATION

In the last step, we mix all model estimates in proportion to their confidence.

$$\mu_t = \sum_{t=1}^{r}\xi^i_{t|t}\mu^i_{t|t}, \tag{27}$$

$$\Sigma_t = \sum_{i=1}^{r}\mu^i_{t|t}[\Sigma^i_{t|t} + (\mu^i_t - \mu_t)(\mu^i_t - \mu_t)^\top]. \tag{28}$$

The position of the target at time t is estimated as $\hat{x}_t = J\mu_t$. Figure 1 shows the flow chart of the proposed algorithm.

V. EXPERIMENTAL VALIDATION

A. CSI FINGERPRINT

In this section, we assess the effectiveness of the indoor localization method we proposed above. We need to obtain the formula for calculating the likelihood function $L_t(x)$ in equation (12) and the Hessian matrix $\nabla^2 L_t\left(\check{x}_t\right)$ in equation (14). The fingerprinting method we use is described in [45]. More precisely, the measurement model can be given by

$$\hat{h}(x) = \sum_{k=1}^{K}\alpha_k exp(-\frac{I^{\frac{1}{3}}}{2}\|x - p_k\|^2). \tag{29}$$

At this point, we can get the analytic expression of equation (13)

$$p(y_t|J\mu_t = x) \simeq \mathcal{N}\left(y_t; \hat{h}\left(x\right), \hat{R}\right) \tag{30}$$

$$= \frac{1}{|2\pi R|^{\frac{1}{2}}} exp[-\frac{1}{2}(y_t - \hat{h}(x))^\top R^{-1}. \times (y_t - \hat{h}(x))]. \tag{31}$$

Then the equation (12) could be written as

$$L_t(x) = logp(y_t|J\mu_t = x) \tag{32}$$

$$\simeq -\frac{1}{2}log|2\pi R| - \frac{1}{2}(y_t - \hat{h}(x))^\top R^{-1}(y_t - \hat{h}(x)). \tag{33}$$

Therefore, the i-th component of its gradient is

$$[\nabla^2 L_t(x)]_i \simeq \frac{\partial\hat{h}(x)^\top}{\partial x_i}R^{-1}(y_t - \hat{h}(x)). \tag{34}$$

Then for equation (14), the (i, j)-th component of the Hessian matrix is

$$\frac{\partial\hat{h}(x)}{\partial x_i} = \sum_{k=1}^{K}\alpha_k\frac{\partial}{\partial x_i}exp(-\frac{I^{\frac{1}{3}}}{2}\|x - p_k\|^2) \tag{35}$$

$$= -\frac{I^{\frac{1}{3}}}{2}\sum_{k=1}^{K}\alpha_k exp(-\frac{I^{\frac{1}{3}}}{2}\|x - p_k\|^2) \times \cdot\frac{\partial}{\partial x_i}(x^\top x - 2p_k^\top x + p_k^\top p_k) \tag{36}$$

$$= I^{\frac{1}{3}}\sum_{k=1}^{K}\alpha_k exp(-\frac{I^{\frac{1}{3}}}{2}\|x - p_k\|^2)(p_k - x)^\top\frac{\partial x}{\partial x_i}, \tag{37}$$

where $\frac{\partial x}{\partial x_1} = [1, 0]^\top$ and $\frac{\partial x}{\partial x_2} = [0, 1]^\top$.

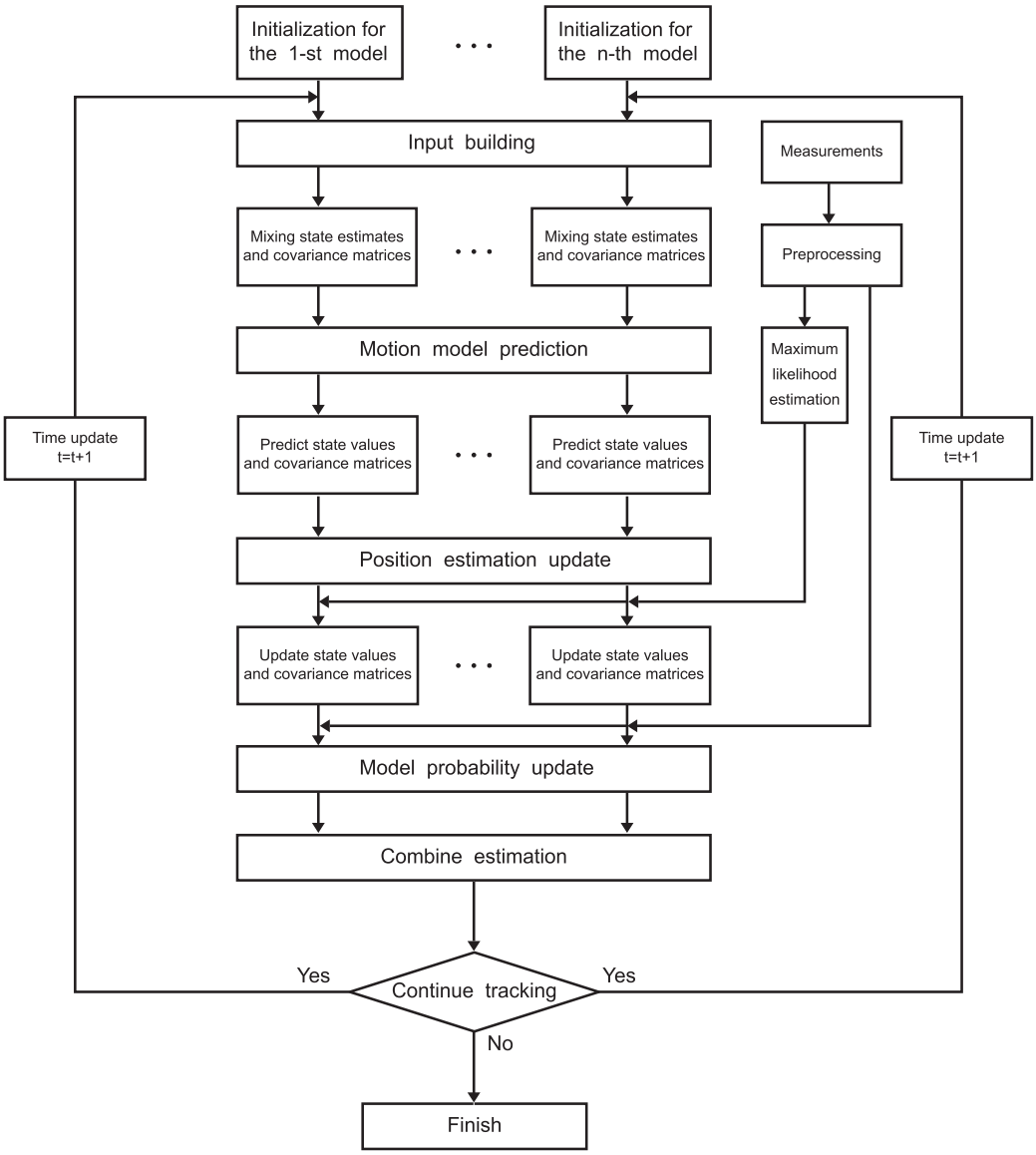

FIGURE 1. Flow chart of the positioning algorithm.

B. ENVIRONMENT SETTING

Currently, obtaining CSI data involves modifying and customizing the kernel of certain hardware. Given the richness of data acquisition, the transmission hardware used in this experiment is a TP-Link WDR4310 router that is pre-installed with the OpenWrt open-source system, as shown in Figure 2. It captures CSI values of 56 subcarriers, using two 10-bit values for each subcarrier's phase and amplitude. Ground truth positions are acquired using motion capture cameras with millimeter level accuracy. Considering the limitations of transmission and reception devices in real-world applications, the transmission end uses 3 antennas while the receiving end uses 1 antenna.

The first experimental environment is set as an empty indoor environment, as shown in Figure 3. In the environment, we selected 70 initialization positions and 26 test positions. After comprehensive consideration of the fingerprint collection workload and positioning accuracy, the distance between the initialization positions is set as 1 meter. To obtain the CSI values sent by the receiver, we use the Ping command to generate a request for the receiver to send a reply, which results in one data packet from the receiver. In this experiment, the Ping command interval is set to 0.1 seconds. This is because the real-time data processing capability of the server-side is limited, and a positioning interval of 0.1 seconds is sufficient to meet the needs of most applications. In order to select the fingerprint feature, we used only amplitude, only unwrapped calibration phase differences (UCPDs) described in [45], both amplitude and UCPDs as fingerprint features for static positioning. The results are shown in Figure 4. As can be seen in the figure, when using CSI amplitude for localization, its localization error is significantly higher than when using phase as the fingerprint feature. When using both phase and amplitude for localization, the

FIGURE 2. The TP-Link WDR4310 router with three antennas used for positioning, with each antenna can receive a set of CSI values of 56 subcarriers.

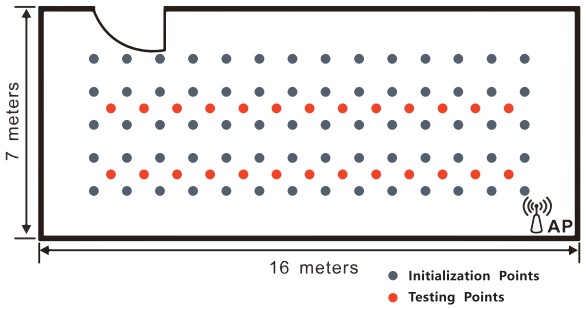

FIGURE 3. The layout and database points of the empty room, where the access point is positioned in the lower-right corner.

localization error is also slightly higher than when using phase alone. In summary, in order to achieve the best localization results, this section only uses phase features, that is, the UCPDs as the fingerprint feature. In static positioning, the average positioning error of using UCPDs as fingerprints is 1.097 meters, while the positioning error of using RSSI as fingerprint features is 3.0824 meters.

Subsequently, we compared the impact of using data from different transmit antennas on the localization results, as shown in Figure 5. As can be seen from the figure, when using three antennas individually for localization, the obtained localization error results are relatively similar, and both are slightly higher than when using data from all three antennas for localization. Therefore, the fingerprints are from all three transmission antennas.

C. TRACKING PERFORMANCE

For the experiment on dynamic targets, we used a robot with a control panel developed by NVIDIA Jetson Nano. The selected motion models are CV and CT models as described in the appendix VI. Considering the possible packet loss during transmission and the need for data preprocessing, the positioning interval is set as $T = 0.5s$. The comparison methods include the MLKF algorithm [45], MLPF algorithm with 50 particles [42], and IMM-EKF [26], IMM-UKF [27]

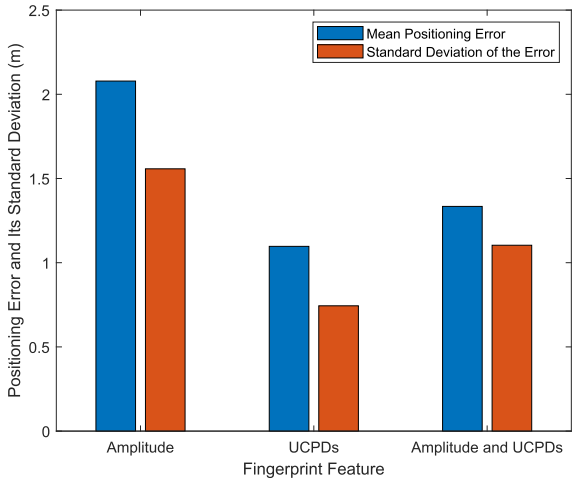

FIGURE 4. Influence of fingerprint feature selection on positioning error.

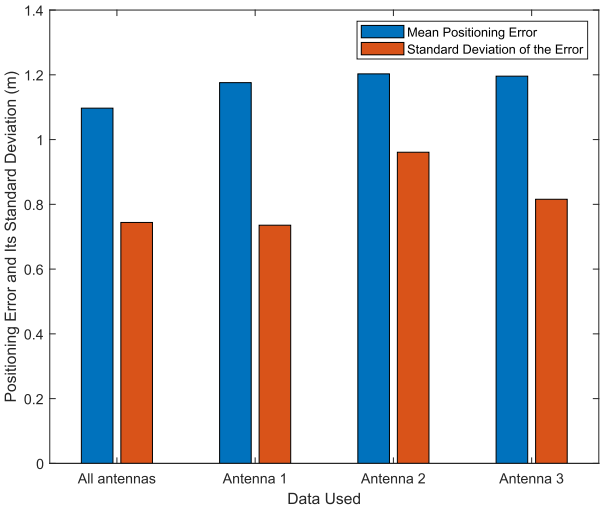

FIGURE 5. Influence of using different transmitting antennas on positioning error.

and IMM-CKF [28] algorithms based on multiple interacting models mentioned earlier. We controlled the target to move along an approximately square path at a constant speed. Firstly, we tested the difference in positioning accuracy between different methods when using the CV and CT models separately and when using interactive multi-modal methods. The results are shown in Figure 6. From the results in the figure, it can be seen that all three selected methods have a certain degree of improvement in positioning accuracy when combined with the interactive multi-modal methods.

The results of the experiment are shown in Table 1. The data in the table shows that the proposed IMM-MLKF algorithm and the MLPF algorithm have a clear advantage in terms of average positioning error compared to other algorithms. The IMM-MLKF algorithm performs better in positioning errors at turns and consumes less computational time in each iteration. The computation time of this method at each iteration is also in the same order of magnitude as other methods, which is significantly better than MLPF. Figure 7 shows the cumulative distribution functions (CDF)

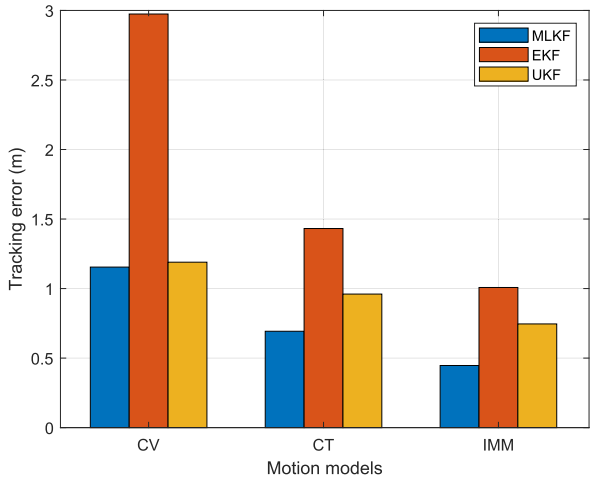

FIGURE 6. Comparison of errors between different motion models.

TABLE 1. Positioning error (empty room).

Methods	Mean Error (m)	Mean Error at Turning Positions (m)	Computation Time (s)
IMM-MLKF	0.4468	0.2760	0.0645
MLKF	0.6930	0.9259	0.0563
MLPF	0.4768	0.6862	0.3408
IMM-EKF	1.0078	0.9984	0.0105
IMM-UKF	0.6723	0.5118	0.0251
IMM-CKF	0.7457	0.7633	0.0204

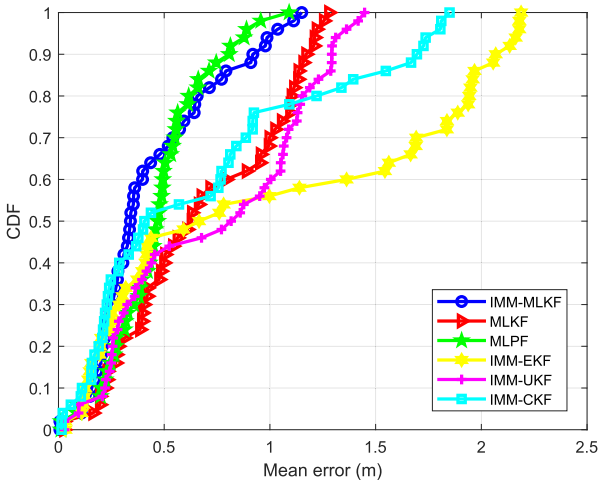

FIGURE 7. Positioning error CDF (empty room).

of distance errors using these methods, and the true trajectory of the object the tracking result of the proposed method is shown in Figure 8.

The second experimental scenario was set up according to a real office environment, shown in Figure 9, where the target starts from the office and moves along the corridor as shown in Figure 10. The results shown in Table 2 indicate that the signal experiences a decline after passing through the wall, affecting the positioning accuracy to some extent. The MLKF method has a large error in this environment. The IMM-UKF and the IMM-MLKF method proposed in this paper have higher positioning accuracy at the turning

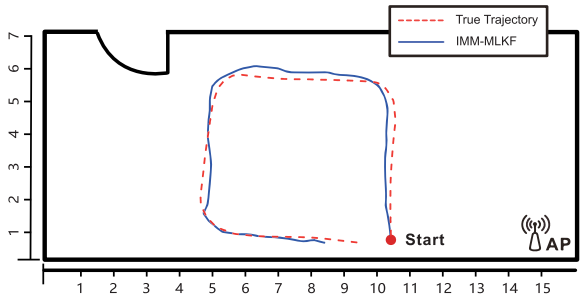

FIGURE 8. Tracking result (empty room).

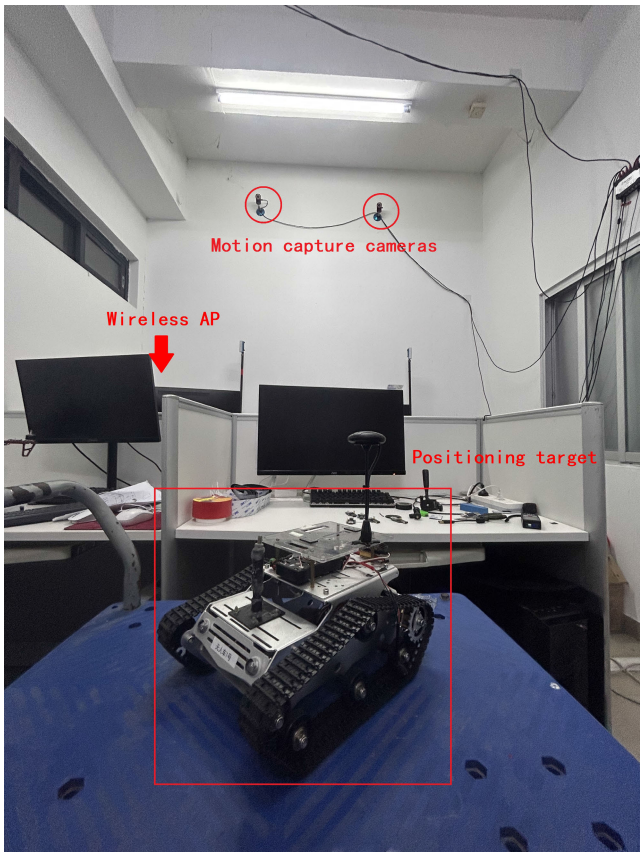

FIGURE 9. The second experimental scenario and the positioning target.

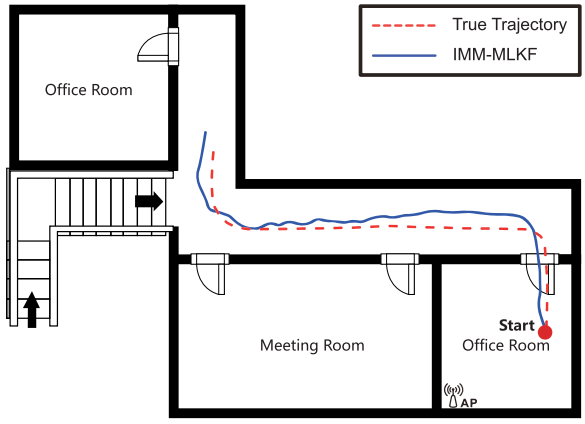

FIGURE 10. Tracking result (office environment).

positions. However, overall, the IMM-MLKF method has better positioning accuracy and its computational speed can

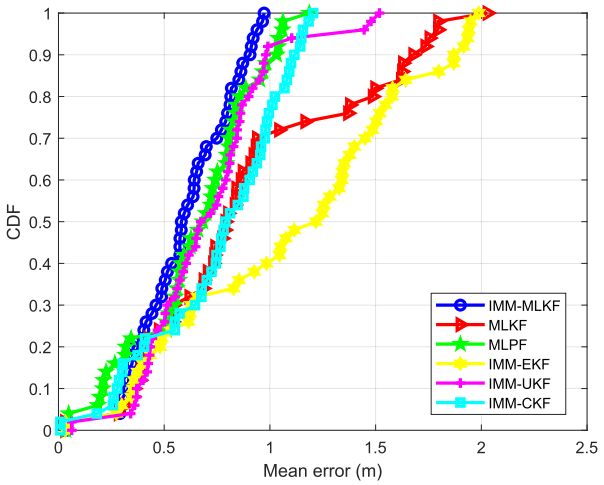

FIGURE 11. Positioning error CDF (Office environment).

TABLE 2. Positioning error (office environment).

Methods	Mean Error (m)	Mean Error at Turning Positions (m)	Computation Time (s)
IMM-MLKF	0.6021	0.5254	0.0705
MLKF	0.9088	1.2493	0.0527
MLPF	0.6484	0.7187	0.5425
IMM-EKF	1.1095	1.0863	0.0151
IMM-UKF	0.7143	0.5649	0.0265
IMM-CKF	0.7623	0.7195	0.0197

still meet the requirements of real-time positioning. The CDF of the mean error is shown in Figure 11.

VI. CONCLUSION

In this paper, we proposed a new positioning method based on the maximum likelihood Kalman filtering, referred to as IMM-MLKF. The core advantage of this method is its ability to adapt to different target movement states by using different motion models, resulting in better positioning results for targets with more complex movement states. Additionally, this method inherits the high computational efficiency of MLKF, allowing it to be applied in real-time positioning. We verified the method through experiments in two different positioning environments, and it has a significant advantage over other similar algorithms when considering the trade-off between positioning accuracy and computational efficiency.

APPENDIX A LINEAR MOTION MODELS

A. CONSTANT VELOCITY MODEL

The constant velocity (CV) model is commonly used to match the situation where the target is moving in a straight line at a constant speed. In Equation (4),

$$F = \begin{bmatrix} 1 & 0 & T & 0 \\ 0 & 1 & 0 & T \\ 0 & 0 & 1 & 0 \\ 0 & 0 & 0 & 1 \end{bmatrix}, \tag{38}$$

and the covariance for the noise w_t is

$$Q = q^2 \begin{bmatrix} \frac{T^3}{3} & \frac{T^2}{2} & 0 & 0 \\ \frac{T^2}{2} & T & 0 & 0 \\ 0 & 0 & \frac{T^3}{3} & \frac{T^2}{2} \\ 0 & 0 & \frac{T^2}{2} & T \end{bmatrix}. \tag{39}$$

B. CONSTANT VELOCITY MODEL

The constant velocity (CT) model is used to simulate the motion of a target undergoing constant angular velocity turning motion. In Equation (4),

$$F = \begin{bmatrix} 1 & \frac{sin(\omega T)}{\omega} & 0 & -\frac{1-cos(\omega T)}{\omega} \\ 0 & cos(\omega T) & 0 & -sin(\omega T) \\ 0 & \frac{1-cos(\omega T)}{\omega} & 1 & \frac{sin(\omega T)}{\omega} \\ 0 & sin(\omega T) & 0 & cos(\omega T) \end{bmatrix}, \tag{40}$$

and the covariance for the noise w_t is

$$Q = q^2 \begin{bmatrix} \frac{T^3}{3} & \frac{T^2}{2} & 0 & 0 \\ \frac{T^2}{2} & T & 0 & 0 \\ 0 & 0 & \frac{T^3}{3} & \frac{T^2}{2} \\ 0 & 0 & \frac{T^2}{2} & T \end{bmatrix}. \tag{41}$$

REFERENCES

[1] T. K. Geok, K. Z. Aung, M. S. Aung, M. T. Soe, A. Abdaziz, C. P. Liew, F. Hossain, C. P. Tso, and W. H. Yong, "Review of indoor positioning: Radio wave technology," *Appl. Sci.*, vol. 11, no. 1, p. 279, Dec. 2020.
[2] C.-M. Own, J. Hou, and W. Tao, "Signal fuse learning method with dual bands WiFi signal measurements in indoor positioning," *IEEE Access*, vol. 7, pp. 131805–131817, 2019.
[3] L. Bai, F. Ciravegna, R. Bond, and M. Mulvenna, "A low cost indoor positioning system using Bluetooth low energy," *IEEE Access*, vol. 8, pp. 136858–136871, 2020.
[4] N. Jing, B. Zhang, and L. Wang, "A novel anchor-free localization method using cross-technology communication for wireless sensor network," *Electronics*, vol. 11, no. 23, p. 4025, Dec. 2022.
[5] M. El-Absi, A. A. Abbas, A. Abuelhaija, F. Zheng, K. Solbach, and T. Kaiser, "High-accuracy indoor localization based on chipless RFID systems at THz band," *IEEE Access*, vol. 6, pp. 54355–54368, 2018.
[6] M. Elsanhoury, P. Mäkelä, J. Koljonen, P. Välisuo, A. Shamsuzzoha, T. Mantere, M. Elmusrati, and H. Kuusniemi, "Precision positioning for smart logistics using ultra-wideband technology-based indoor navigation: A review," *IEEE Access*, vol. 10, pp. 44413–44445, 2022.
[7] A. D. Firoozabadi, C. Azurdia-Meza, I. Soto, F. Seguel, N. Krommenacker, D. Iturralde, P. Charpentier, and D. Zabala-Blanco, "A novel frequency domain visible light communication (VLC) three-dimensional trilateration system for localization in underground mining," *Appl. Sci.*, vol. 9, no. 7, p. 1488, Apr. 2019.
[8] F. Liu, J. Liu, Y. Yin, W. Wang, D. Hu, P. Chen, and Q. Niu, "Survey on WiFi-based indoor positioning techniques," *IET Commun.*, vol. 14, no. 9, pp. 1372–1383, Jun. 2020.
[9] Z. Yang, Z. Zhou, and Y. Liu, "From RSSI to CSI: Indoor localization via channel response," *ACM Comput. Surv.*, vol. 46, no. 2, pp. 1–32, Nov. 2013.
[10] J. M. Rocamora, I. W.-H. Ho, W. Mak, and A. P. Lau, "Survey of CSI fingerprinting-based indoor positioning and mobility tracking systems," *IET Signal Process.*, vol. 14, no. 7, pp. 407–419, Sep. 2020.
[11] A. Makki, A. Siddig, M. Saad, and C. Bleakley, "Survey of WiFi positioning using time-based techniques," *Comput. Netw.*, vol. 88, pp. 218–233, Sep. 2015.
[12] C. Basri and A. E. Khadimi, "Survey on indoor localization system and recent advances of WiFi fingerprinting technique," in *Proc. 5th Int. Conf. Multimedia Comput. Syst. (ICMCS)*, Sep. 2016, pp. 253–259.
[13] K. Wu, J. Xiao, Y. Yi, D. Chen, X. Luo, and L. M. Ni, "CSI-based indoor localization," *IEEE Trans. Parallel Distrib. Syst.*, vol. 24, no. 7, pp. 1300–1309, Jul. 2013.

[14] W. Liu, Q. Cheng, Z. Deng, H. Chen, X. Fu, X. Zheng, S. Zheng, C. Chen, and S. Wang, "Survey on CSI-based indoor positioning systems and recent advances," in *Proc. Int. Conf. Indoor Positioning Indoor Navigat. (IPIN)*, Sep. 2019, pp. 1–8.
[15] Z. Chen, "Bayesian filtering: From Kalman filters to particle filters, and beyond," *Statistics*, vol. 182, no. 1, pp. 1–69, 2003.
[16] S. Monica and F. Bergenti, "Hybrid indoor localization using WiFi and UWB technologies," *Electronics*, vol. 8, no. 3, p. 334, Mar. 2019.
[17] S. Subedi, D.-H. Kim, B.-H. Kim, and J.-Y. Pyun, "Improved smartphone-based indoor localization system using lightweight fingerprinting and inertial sensors," *IEEE Access*, vol. 9, pp. 53343–53357, 2021.
[18] X. Wang, M. Jiang, Z. Guo, N. Hu, Z. Sun, and J. Liu, "An indoor positioning method for smartphones using landmarks and PDR," *Sensors*, vol. 16, no. 12, p. 2135, Dec. 2016.
[19] Y. Shen, B. Hwang, and J. P. Jeong, "Particle filtering-based indoor positioning system for beacon tag tracking," *IEEE Access*, vol. 8, pp. 226445–226460, 2020.
[20] B. G. Sileshi, C. Ferrer, and J. Oliver, "Particle filters and resampling techniques: Importance in computational complexity analysis," in *Proc. Conf. Design Architectures Signal Image Process.*, Oct. 2013, pp. 319–325.
[21] J. M. Castro-Arvizu, J. Vilà-Valls, A. Moragrega, P. Closas, and J. A. Fernandez-Rubio, "Received signal strength–based indoor localization using a robust interacting multiple model–extended Kalman filter algorithm," *Int. J. Distrib. Sensor Netw.*, vol. 13, no. 8, 2017, Art. no. 1550147717722158.
[22] Z. Cai, L. Shang, D. Gao, K. Zhao, and Y. Wang, "Indoor mobile localization in mixed environment with RSS measurements," *Int. J. Distrib. Sensor Netw.*, vol. 11, no. 5, May 2015, Art. no. 106475.
[23] I. Arasaratnam and S. Haykin, "Cubature Kalman filters," *IEEE Trans. Autom. Control*, vol. 54, no. 6, pp. 1254–1269, Jun. 2009.
[24] R. Murray-Smith and T. Johansen, *Multiple Model Approaches to Nonlinear Modelling and Control*. Boca Raton, FL, USA: CRC Press, 2020.
[25] E. Mazor, A. Averbuch, Y. Bar-Shalom, and J. Dayan, "Interacting multiple model methods in target tracking: A survey," *IEEE Trans. Aerosp. Electron. Syst.*, vol. 34, no. 1, pp. 103–123, Jan. 1998.
[26] Y. Zhang, W. Fu, D. Wei, J. Jiang, and B. Yang, "Moving target localization in indoor wireless sensor networks mixed with LOS/NLOS situations," *EURASIP J. Wireless Commun. Netw.*, vol. 2013, no. 1, pp. 1–10, Dec. 2013.
[27] D. Lee, C. Liu, and J. K. Hedrick, "Interacting multiple model-based human motion prediction for motion planning of companion robots," in *Proc. IEEE Int. Symp. Saf., Secur., Rescue Robot. (SSRR)*, Oct. 2015, pp. 1–7.
[28] M. N. Radhika, S. S. Parthasarathy, and M. Mallick, "IMM-CKF and posterior Cramér–Rao lower bound for a highly maneuvering target," *Solid State Technol.*, vol. 63, no. 4, pp. 1591–1607, 2020.
[29] A. Sobehy, É. Renault, and P. Mühlethaler, "CSI-MIMO: K-nearest neighbor applied to indoor localization," in *Proc. IEEE Int. Conf. Commun. (ICC)*, Jun. 2020, pp. 1–6.
[30] Z. Hao, Y. Yan, X. Dang, and C. Shao, "Endpoints-clipping CSI amplitude for SVM-based indoor localization," *Sensors*, vol. 19, no. 17, p. 3689, Aug. 2019.
[31] O. Altay and M. Ulas, "Location determination by processing signal strength of Wi-Fi routers in the indoor environment with linear discriminant classifier," in *Proc. 6th Int. Symp. Digit. Forensic Secur. (ISDFS)*, Mar. 2018, pp. 1–4.
[32] X. Wang, L. Gao, S. Mao, and S. Pandey, "DeepFi: Deep learning for indoor fingerprinting using channel state information," in *Proc. IEEE Wireless Commun. Netw. Conf. (WCNC)*, Mar. 2015, pp. 1666–1671.
[33] F. Qin, T. Zuo, and X. Wang, "CCpos: WiFi fingerprint indoor positioning system based on CDAE-CNN," *Sensors*, vol. 21, no. 4, p. 1114, Feb. 2021.
[34] W. Sun, M. Xue, H. Yu, H. Tang, and A. Lin, "Augmentation of fingerprints for indoor WiFi localization based on Gaussian process regression," *IEEE Trans. Veh. Technol.*, vol. 67, no. 11, pp. 10896–10905, Nov. 2018.
[35] J. Bi, M. Zhao, G. Yao, H. Cao, Y. Feng, H. Jiang, and D. Chai, "PSOSVR-Pos: WiFi indoor positioning using SVR optimized by PSO," *Expert Syst. Appl.*, vol. 222, Jul. 2023, Art. no. 119778.
[36] D. Dardari, P. Closas, and P. M. Djurić, "Indoor tracking: Theory, methods, and technologies," *IEEE Trans. Veh. Technol.*, vol. 64, no. 4, pp. 1263–1278, Apr. 2015.
[37] S.-H. Lee, I.-K. Lim, and J.-K. Lee, "Method for improving indoor positioning accuracy using extended Kalman filter," *Mobile Inf. Syst.*, vol. 2016, pp. 1–15, Jun. 2016.
[38] S. J. Julier and J. K. Uhlmann, "Unscented filtering and nonlinear estimation," *Proc. IEEE*, vol. 92, no. 3, pp. 401–422, Mar. 2004.
[39] C. Liu, P. Shui, and S. Li, "Unscented extended Kalman filter for target tracking," *J. Syst. Eng. Electron.*, vol. 22, no. 2, pp. 188–192, Apr. 2011.
[40] S. Konatowski, P. Kaniewski, and J. Matuszewski, "Comparison of estimation accuracy of EKF, UKF and PF filters," *Annu. Navigat.*, vol. 23, no. 1, pp. 69–87, Dec. 2016.
[41] D. Marelli, M. Fu, and B. Ninness, "Asymptotic optimality of the maximum-likelihood Kalman filter for Bayesian tracking with multiple nonlinear sensors," *IEEE Trans. Signal Process.*, vol. 63, no. 17, pp. 4502–4515, Sep. 2015.
[42] W. Wang, D. Marelli, and M. Fu, "Dynamic indoor localization using maximum likelihood particle filtering," *Sensors*, vol. 21, no. 4, p. 1090, Feb. 2021.
[43] S. Vasuhi and V. Vaidehi, "Target tracking using interactive multiple model for wireless sensor network," *Inf. Fusion*, vol. 27, pp. 41–53, Jan. 2016.
[44] W. Wang, D. Marelli, and M. Fu, "Multiple-vehicle localization using maximum likelihood Kalman filtering and ultra-wideband signals," *IEEE Sensors J.*, vol. 21, no. 4, pp. 4949–4956, Feb. 2021.
[45] W. Wang, D. Marelli, and M. Fu, "Fingerprinting-based indoor localization using interpolated preprocessed CSI phases and Bayesian tracking," *Sensors*, vol. 20, no. 10, p. 2854, May 2020.

WENXU WANG received the bachelor's and master's degrees from Northwestern Polytechnical University, in 2012 and 2015, respectively, and the Ph.D. degree from the Guangdong University of Technology, in 2021. Since 2022, he has been an Assistant Professor with the School of Information Engineering, Shaoguan University, mainly conducting research on indoor positioning, target tracking, and other related fields.

YINGBIAO JIA received the Ph.D. degree in information and communication engineering from the School of Electronics and Information Engineering, Northwestern Polytechnical University, in December 2014. He is currently a Lecturer with the Department of Communication Engineering, School of Information Engineering, Shaoguan University. His main research interests include signal processing and wireless communications.